Neurosci Bull June 1, 2011, 27(3): 173–184. http://www.neurosci.cn
DOI: 10.1007/s12264-011-1044-2

·Original Article·

Neural circuit and its functional roles in cerebellar cortex

Lei WANG, Shen-Quan LIU

Department of Mathematics, South China University of Technology, Guangzhou 510640, China

Abstract: **Objective** To investigate the spike activities of cerebellar cortical cells in a computational network model constructed based on the anatomical structure of cerebellar cortex. **Methods and Results** The multicompartment model of neuron and NEURON software were used to study the external influences on cerebellar cortical cells. Various potential spike patterns in these cells were obtained. By analyzing the impacts of different incoming stimuli on the potential spike of Purkinje cell, temporal focusing caused by the granule cell-golgi cell feedback inhibitory loop to Purkinje cell and spatial focusing caused by the parallel fiber-basket/stellate cell local inhibitory loop to Purkinje cell were discussed. Finally, the motor learning process of rabbit eye blink conditioned reflex was demonstrated in this model. The simulation results showed that when the afferent from climbing fiber existed, rabbit adaptation to eye blinking gradually became stable under the Spike Timing-Dependent Plasticity (STDP) learning rule. **Conclusion** The constructed cerebellar cortex network is a reliable and feasible model. The model simulation results confirmed the output signal stability of cerebellar cortex after STDP learning and the network can execute the function of spatial and temporal focusing.

Keywords: computational network model; cerebellar cortex; temporal focusing; spatial focusing; Spike Timing-Dependent Plasticity; eye blink conditioned reflex

1 Introduction

Cerebellar cortex is closely associated with motor learning[1]. Its functional structure and neural circuits are very simple. There are 5 types of cerebellar cortical cells, including Purkinje cell, granule cell, basket cell, stellate cell and golgi cell, among which Purkinje cell is the principal type in the cortex and the other types are local interneurons[2,3]. Mossy fibers and climbing fibers are excitatory afferent fibers that use excitatory amino acids, and they play an excitatory role on Purkinje cells and granule cells, respectively. All the interneurons except the granule cell release neurotransmitter γ-aminobutyric acid (GABA), and therefore are inhibitory cells[4].

The complex peak potential caused by the afferent of climbing fibers can lead to a long-term reduction in synaptic transmission between parallel fiber and Purkinje cell. Long-term synaptic plasticity variation in this kind of synaptic function is the neural basis for cerebellar motor learning. It is widely proposed that the climbing fibers signal errors in motor performance, either in the usual manner of discharge frequency modulation or as a single announcement of an "unexpected event"[2,5].

Golgi cells are inhibitory interneurons located within the granule cell layer. They usually receive excitatory input from parallel fibers, and then inhibit granule cells. This simple feedback inhibition can remove the excitatory affer-

Corresponding author: Shen-Quan LIU
Tel: +86-20-87114815; Fax: +86-20-87110446
E-mail: mashqliu@scut.edu.cn
Article ID: 1673-7067(2011)03-0173-12
Received date: 2010-11-12; Accepted date: 2011-02-16

ent from granule cells/parallel fibers to Purkinje cells and restrict further excitement of Purkinje cells, which plays a role in the formation of temporal focusing[6].

Basket cells and stellate cells, the molecular layer inhibitory interneurons, can also receive excitatory afferents from parallel fibers. Their axons unfold to both sides of the parallel fibers and form inhibitory synaptic connections with Purkinje cells of the 2 sides. Consequently, when a row of Purkinje cells are excited by a bunch of parallel fiber forming an excitement area parallel to the leaf, the peripheral suppression function aroused by basket cells and stellate cells would induce space confinement of the excitatory response of Purkinje cells caused by the mossy fiber afferents, process of which is known as the spatial focusing effect. The spatial and temporal focusing in cerebellar cortex caused by interneurons would have great significance on the coordination of muscle movement in space and time[6].

The cerebellar cortex has long been described as the best anatomically and physiologically understood circuit in the mammalian central nervous system. It has been widely studied in many facets, such as its structure and function[7-11], the motor learning and long-term potential (LTP)/long-term depression (LTD) phenomena on cerebellar cortex[12-15], and the oscillation and synchrony phenomena in cerebellum[16-19]. Since most models employed in previous studies were only parts of the structure or small circuits in cerebellar cortex, it is necessary to construct a whole cerebellar cortex network model, which contains all the small circuits and reflects some typical properties of cerebellar cortex. The present study aimed to establish this network model based on the anatomy of cerebellar cortex, by adding the synaptic connections into the compartment models of Purkinje cells, granule cells, basket cells, stellate cells and golgi cells in cerebellar cortex.

2 Materials and methods

The constructed cerebellar cortex network model contained totally 90 cells, including 5 Purkinje cells, 50 granule cells, 10 basket cells, 10 stellate cells, 5 golgi cells, 5 mossy fibers and 5 climbing fibers. As shown in Fig. 1, each mossy fiber was connected with 10 granule cells, corresponding to the high-frequency stimulation input. Each granule cell could form 2 parallel fibers, and thus 50 granule cells could form a total of 100 parallel fibers in the network. For the glogi cells, each cell could receive excitatory afferent from 20 parallel fibers, and every 10 granule cells would receive feedback inhibition from one golgi cell. For the Purkinje cells, each cell had 100 dendrite spines, through which the cell receives excitatory afferent from parallel fibers, while each parallel fiber could only form a single synaptic connection with one Purkinje cell. For the stellate cells and basket cells, each could receive excitatory input from 10 parallel fibers, and every 2 stellate cells and 2 basket cells would inhibit one Purkinje cell. Besides, connection was not made between cells of the same kind, such as granule cell to granule cell, because this kind of connection has little influence on the whole network activities in the cerebellar cortex model.

The network connection among the cells and fibers in cerebellar cortex were as follows: mossy fibers and climbing fibers received an external stimulus and then excited granule cells and Purkinje cells, respectively. Granule cells excited golgi cells' dendrites through parallel fibers, and then golgi cells gave a feedback inhibitory signal to granule cells through the axon-dendrite synapse. Besides, parallel fibers excited the top of Purkinje dendritic spines and basket/stellate cells' dendrites, while axons of basket/stellate cells in turn inhibited Purkinje cell's soma and dendrites. These neurons and synaptic connections constituted the entire cerebellar cortex network here. The hierarchy of neuronal structure in cerebellar cortex network was simple and clear, with each cell's structure being in order. Based on the anatomy of the cerebellar cortex[2,4], the specific ion channels in Purkinje cells, golgi cells and granule cells[20-22], and the detailed synaptic connections between cerebellar cortical cells[5], the cerebellar cortex network model was constructed. This model was very close to the natural structure of the cerebellar cortex. The circuit of cerebellar cortex could be modulated and the excitatory afferent into cells could be controlled (Fig. 1).

In the theoretical analysis of network model, a single

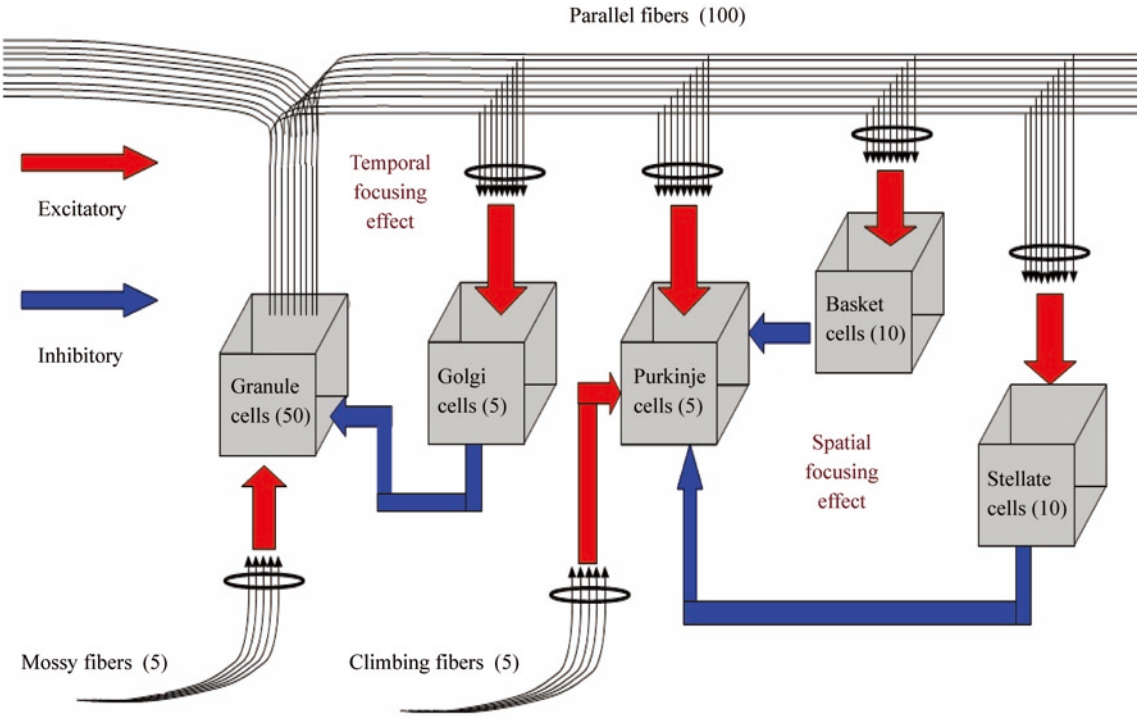

Fig. 1 An illustration of the cerebellar cortex network model, which was comprised of 90 cells, including 5 Purkinje cells, 50 granule cells, 10 basket cells, 10 stellate cells, 5 golgi cells, 5 mossy fibers and 5 climbing fibers. Red arrows indicated excitatory input, while blue arrows indicated inhibitory input.

cell is described by Conductance-based models and morphology of each cell is characterized by the compartment model, such as one Purkinje cell having 3 parts including soma, smooth dendrite and spiny dendrite. According to the different morphological characteristics, here different compartment numbers were used to describe the different parts of neuron. For granule cells, golgi cells, stellate cells and basket cells, the same method was used as Purkinje cells. The basic theory of electrical signal transmission within cells was Rall's cable model and its discrete format was neuronal compartment model. The description of a compartment was just like that of a membrane structure, additional to different ion channels. The connection between different compartments in a single cell was a discrete format of Rall's cable model. Taking all these features together, the potential activities of different cells could be obtained. According to the previous reports[20-24], the ion channels in different cell's compartments were different, and the specific parameters and neuronal equations were described as follows:

$$\begin{cases} C\dfrac{\mathrm{d}V}{\mathrm{d}t} = I_{\text{ion}} + I(t) + I_{\text{compartment}} + I_{\text{syn}} \\ \dfrac{\mathrm{d}x}{\mathrm{d}t} = (x_{\infty} - x)/\tau_x \end{cases} \quad (1)$$

In the equations, C represented cell membrane capacitance and $x = x(V)$ represented the open status of different ion channels. $I(t)$ represented the strength of an external stimulus, and $I_{\text{compartment}}$ and I_{syn} represented the compartment currents and synaptic currents (syn=GABA, AMPA and NMDA), respectively. Strength of alterating current (AC) stimulation was indicated as B+Acos(wt). The compartment interchange currents were calculated as the following: $I_{\text{compartment}} = \dfrac{V_{i+1} - V_i}{R_{i+1}} + \dfrac{V_{i-1} - V_i}{R_{i-1}}$, where R_i represented the connection strength between the 2 adjoin compartments.

Chemical synapses were used to describe the connections between cells. If cell B was excited by cell A, the NMDA- and AMPA-type excitatory synaptic currents were

added on the receiving end of cell B. On the other hand, if cell A was inhibited by cell B, the GABA-type inhibitory synaptic currents were added on the receiving end of cell A. The specific connection strength was characterized by the strength of their excitation or inhibition (Table 1). The 3 kinds of expression of synaptic connection used in this model were adopted from a previous report[24], as listed in the following:

(1) GABA synaptic currents: $I_{GABA}= g_{GABA}\times[\exp(-t / \tau_2) - \exp(-t / \tau_1)](V-E_{GABA})$, where τ_1 and τ_2 represented the rising and falling time of synapse, respectively, and E_{GABA} indicated the reversal potential. g_{GABA} represented the maximal inhibitory synaptic strength.

(2) AMPA synaptic currents: $I_{AMPA}= g_{AMPA} \times\exp(-t / \tau)(V-E_{AMPA})$, where τ represented the delay time constant of synapse, and E_{AMPA} was the reversal potential. g_{AMPA} was the maximal excitatory synaptic strength.

(3) NMDA synaptic currents: $I_{NMDA}= g_{NMDA}\times[Mg^{2+}](Ron+Roff)(V-E_{NMDA})$, where E_{NMDA} was the reversal potential, and g_{NMDA} was the maximal excitatory synaptic strength. $[Mg^{2+}] = 1/[1+\exp(-0.062V)/3.57]$, representing Mg^{2+} concentration. $Ron' = -Ron/2.6$, $Roff' = -0.035Roff$, representing the state variables of channels, respectively. Some specific parameters in the above equations were as follows: $\tau_1 = 1$ ms, $\tau_2 = 200$ ms, $E_{GABA} = -80$ mV, $E_{AMPA} = 0$ mV, $E_{NMDA} = 0$ mV.

For Purkinje cell, the specific parameters and expression of each ionic current could be found in a previous report[20]. For golgi cell, the specific parameters and expression of each ionic current could also be found in published reports[21,22]. For stellate/basket cell, mossy fiber and climbing fiber, Na^+ and K^+ were used in the Hodgkin-Huxley equations. The specific parameters and expression had been published[23]. For granule cell, the specific parameters and expression had been reported by Migliore M *et al.*[24].

The cerebellar cortex network model was constructed by NEURON software[25], and data processing was conducted using ORGIN and MATLAB softwares. The simulation results were repeatedly verified.

3 Simulation results

3.1 The corresponding responses of Purkinje cell to different afferent fibers The whole cerebellar cortex network model contained 2 kinds of inputs: mossy fiber afferents and climbing fiber afferents. As shown in Fig. 2, different kinds of stimulations caused different firing patterns of Purkinje cell in cerebellar cortex. Purkinje cells produced a high-frequency phenomenon and a low-frequency

Table 1. Synaptic connection strength between cells and fibers (mS/cm^2)

Cell and fibers	Purkinje cell	Granule cell	Golgi cell	Basket cell	Stellate cell	Mossy fiber	Climbing fiber
Purkinje cell	–	–	–	–	–	–	–
Granule cell	NMDA:0.0007 AMPA:0.0002	–	NMDA:0.0021 AMPA:0.0006	NMDA:0.0105 AMPA:0.003	NMDA:0.0105 AMPA:0.003	–	–
Golgi cell	–	GABA:0.00013	–	–	–	–	–
Basket cell	GABA:0.00001	–	–	–	–	–	–
Stellate cell	GABA:0.00005	–	–	–	–	–	–
Mossy fiber	–	NMDA:0.00175 AMPA:0.0005	–	–	–	–	–
Climbing fiber	NMDA:0.007 AMPA:0.002	–	–	–	–	–	–

Note: The values were synaptic connection strength between cells and fibers. The strength was chosen to be proper values to get the whole activities of cerebellar cortical cells. The synapse connection direction was from cells or fibers in the column to cells or fibers in the row. NMDA denoted the synaptic conductance in NMDA synaptic expression, and AMPA denoted the synaptic conductance in AMPA synaptic expression. GABA denoted the synaptic conductance in GABA synaptic expression.

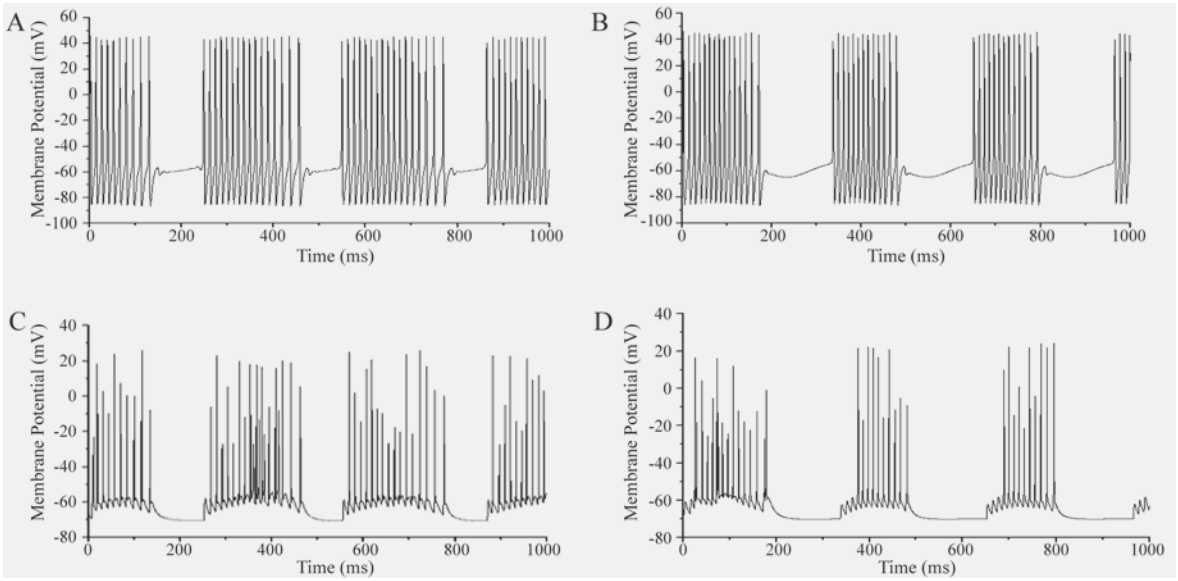

Fig. 2 Action potential maps of afferent fibers and Purkinje cell. A: mossy fiber; B. climbing fiber; C. Purkinje cell when only the mossy fiber was stimulated; D. Purkinje cell when only the climbing fiber was stimulated. The strength of stimulation to mossy fiber was [0.07+0.03×cos(0.02t)] nA, while the stimulation to climbing fiber was [0.07+0.06×sin(0.02t)] nA. Duration: 1 000 ms. Different kinds of stimulations could cause different firing patterns of Purkinje cell in cerebellar cortex.

phenomenon in response to 2 different afferent fibers, which was consistent with the finding that mossy fibers are the primary afferent system and they can induce a higher firing rate of Purkinje cell, while climbing fibers can cause Purkinje cell to display a relatively lower firing rate[2,5].

3.2 Action potential maps of cerebellar cortical cells Mossy fibers and climbing fibers were simultaneously stimulated, and the action potential maps of the 5 kinds of cells in cerebellar cortex network were recorded. As shown in Fig. 3, the spike patterns of cerebellar cortical cells were diverse. For a given stimulus, different kinds of cells produced different responses and firing patterns. The spike patterns of Purkinje cell were not only dense but also complex, resulting in the disorder of action potential. All these spiking patterns demonstrated the sensitivity of cerebellar cortical network to external stimulation.

3.3 Temporal focusing effect The temporal focusing effect is a phenomenon caused by the feedback inhibition from golgi cells to granule cells, and this kind of inhibition can restrict the further excitement of Purkinje cells. Fig. 4 showed the Purkinje cell action potential maps caused by the feedback inhibition from golgi cells to granule cells, with feedback inhibition strength being 13 (Fig. 4A), 38 (Fig. 4B), or 73 μS/cm^2 (Fig. 4C).

As shown in Fig. 4D, with the increase in inhibition strength of golgi cells to granule cells, the mean firing rate of Purkinje cell showed a clear tendency of decrease. This was due to the existence of such a feedback inhibition loop of golgi cells and granule cells, which could induce the activation of Purkinje cells to be confined in temporal. This could also explain the temporal focusing effect in cerebellar cortical network.

3.4 Spatial focusing effect The spatial focusing effect is a phenomenon caused by the existence of inhibition loop from basket/stellate cells to Purkinje cells. By this effect, excitatory responses of Purkinje cells caused by the afferent impulses from mossy fibers through granule cells to parallel fibers are confined in spatial.

Fig. 5A showed the constructed morphological diagram of Purkinje cell, which was simplified from the original diagram published previously[26]. Purkinje cells with different inhibited regions were shown in Fig. 5B–E, in which yellow color represented the inhibitory region of Purkinje cell dendrites, and black color represented the excitatory region of Purkinje cell dendrites.

As shown in Fig. 5F, with the increase in the percent-

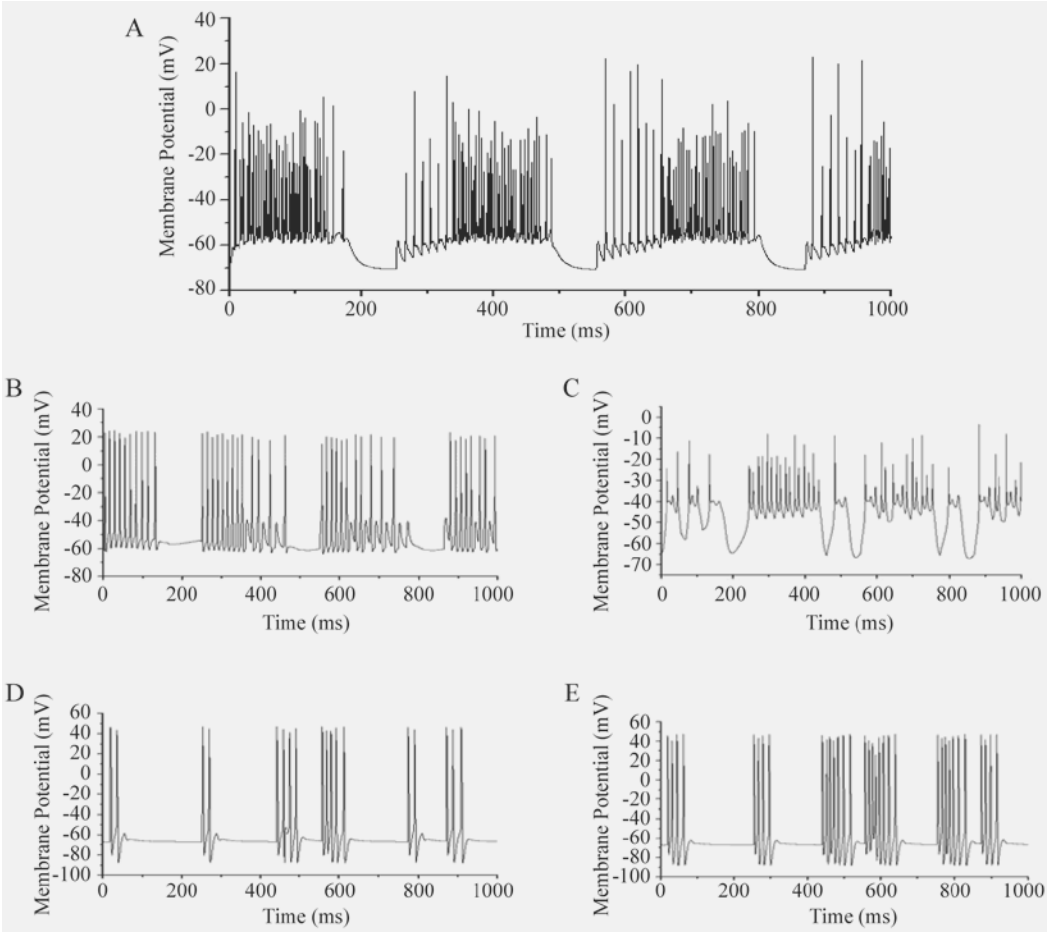

Fig. 3 Action potential maps of different cells. A: Purkinje cell; B: granule cell; C: golgi cell; D: basket cell; E: stellate cell. The strength of stimulation to mossy fiber was [0.07+0.03×cos(0.02t)] nA, while the stimulation to climbing fiber was [0.07+0.06×sin(0.02t)] nA. Duration: 1 000 ms.

age of inhibited region, the mean firing rate of Purkinje cells decreased, indicating that the local inhibitory effect on Purkinje cell dendrites caused by stellate cells and basket cells could effectively regulate Purkinje cell's response. That is to say, the excitatory afferent to Purkinje cell was limited in space, which could also explain the spatial focusing effect in cerebellar cortical network.

3.5 Model reflection of rabbit eye blink conditioned reflex To realize the process of rabbit eye blink conditioned reflex in the present network model, here a diagram modeling this process was constructed, and Spike Timing-Dependent Plasticity (STDP) learning rule was added on the synapse of parallel fibers to Purkinje cells[27,28] (Fig. 6).

In Fig. 6, the ring tone represented the stimulation to mossy fibers (unconditioned stimulus), and air blow represented the stimulation to climbing fibers (conditioned stimulus). Firstly, the afferent of climbing fibers was fixed, and then the parallel fiber-to-Purkinje cell synapses took a learning process under STDP learning rule. When the learning times reached a certain number, the response of Purkinje cell would be stable and the STDP learning process of rabbit eye blink conditioned reflex was completed. Next, climbing fibers were removed, and the response of Purkinje cells was little changed, which indicated that the rabbit could still make eye blinking movements when hearing the ring tone.

There were 2 kinds of excitatory synaptic connections between parallel fibers and Purkinje cells in the present model, including AMPA-type synapse and NMDA-type synapse. The maximal synaptic conductances (g) of the

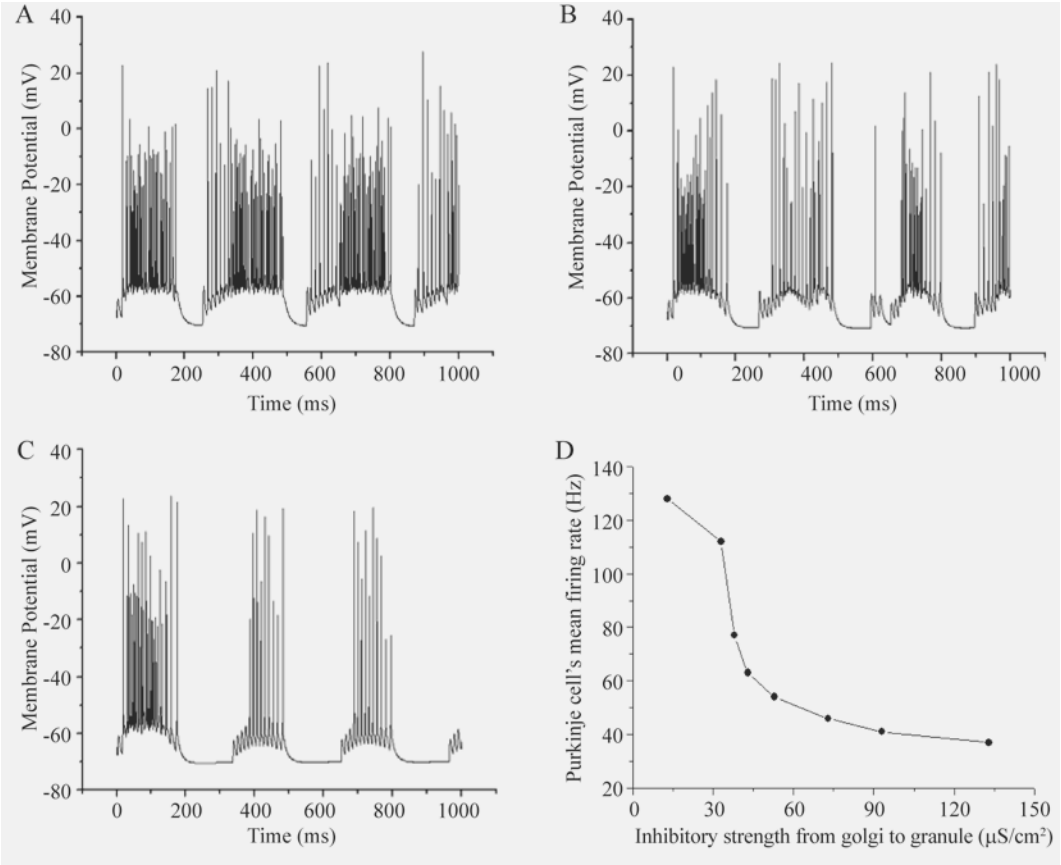

Fig. 4 The Purkinje cell action potential maps caused by the feedback inhibition from golgi cells to granule cells, with feedback inhibition strength of 13 (A), 38 (B) or 73 μS/cm^2 (C). D: The relationship between inhibition strength from golgi cells to granule cells and the mean firing rate of Purkinje cells. The strength of stimulation to mossy fiber was [0.07+0.03×cos(0.02t)] nA, while the stimulation to climbing fiber was [0.07+0.06×sin(0.02t)] nA. Duration: 1 000 ms.

AMPA-type and NMDA-type synapses were indicated as g_{APMA} and g_{NMDA}, respectively.

To determine the maximal synaptic conductance (g) of the simulated STDP synapse, the STDP learning rule was used. This was accurate if the time between presented spike pairs was longer compared to the time between spikes in the pair. To avoid runaway behavior, the additive rule was applied to an intermediate g_{raw} that was then filtered through a sigmoid function. In particular, the change of Δg_{raw} in synaptic strength is given by:

$$\Delta g_{\mathrm{raw}} = \begin{cases} A_+ \dfrac{\Delta t-\tau_0}{\tau_+} e^{-(\Delta t-\tau_0)/\tau_+}, & for\ \Delta t > \tau_0 \\ A_- \dfrac{\Delta t-\tau_0}{\tau_-} e^{(\Delta t-\tau_0)/\tau_-}, & for\ \Delta t < \tau_0 \end{cases} \quad (2)$$

$$g_{\mathrm{raw\_i+1}} = g_{\mathrm{raw\_i}} + \Delta g_{\mathrm{raw}}, \mathrm{i} = 0, 1, \cdots \quad (3)$$

where $\Delta t = t_{\mathrm{post}} - t_{\mathrm{pre}}$, indicating the difference in postsynaptic and presynaptic spike times. The parameters τ_+ and τ_- determined the width of the learning windows for potentiation and depression respectively. The amplitudes A_+ and A_- determined the magnitude of synaptic change per spike pair. The shift τ_0 reflected the finite time of information transport through the synapse. g_{raw} was an intermediate variable, which connected the relationship between g and g_{raw}. The parameters were as follows: A_+ = 8 ms, τ_+ = 80 ms, A_- = 20 ms, τ_- = 120 ms, τ_0 = 0.6 ms, $g_{\mathrm{mid}} = g_{\mathrm{slope}} = \dfrac{g_{\max}}{2} = 5$. The initial value of g_{raw} was 0.31 ms. The raw synaptic strength was then filtered according to the following equation: $g = \dfrac{g_{\max}}{2}(\tanh(\dfrac{g_{\max} - g_{\mathrm{mid}}}{g_{\mathrm{slope}}}) + 1)$. We could get $g_{N+1} = g_N + \Delta g$, where N denotes the times of learning.

From the expression of Δg_{raw} and g, it could be seen that in the condition of $\Delta t > \tau_0$, the change of Δg_{raw} was positive, while in the condition of $\Delta t < \tau_0$, the change of Δg_{raw}

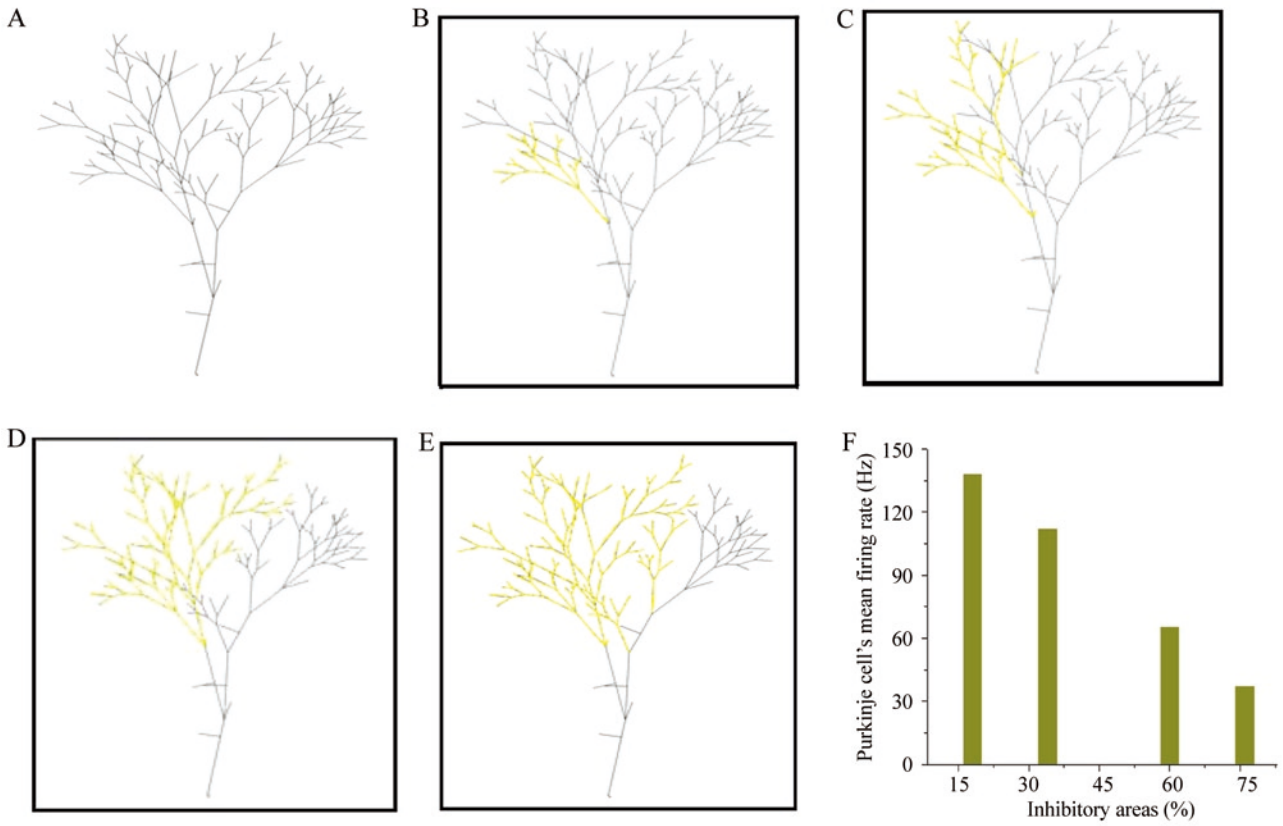

Fig. 5 A: A morphological diagram of Purkinje cell in the present cerebellar cortex network model. B-E: Purkinje cells with different inhibited regions. Yellow color represented the inhibitory region of Purkinje cell dendrites, and black color represented the excitatory region of Purkinje cell dendrites. F: The relationship between the percentage of inhibited region of dendrites to the total area and the corresponding mean firing rate of Purkinje cells. The strength of stimulation to mossy fiber was [0.07+0.03×cos(0.02t)] nA, while the strength of stimulation to climbing fiber was [0.07+0.06×sin(0.02t)] nA. Duration: 1 000 ms.

was negative. If Δt continued increasing in the condition of $\Delta t > \tau_0$, Δg would continue increasing, and LTP would be generated. Conversely, if Δt continued decreasing when $\Delta t < \tau_0$, Δg would continue decreasing, and LTD would be generated.

Based on the above STDP learning rule, and with the aid of NEURON and MATLAB softwares, conclusion was drawn from our simulation that when the times of learning reached 7, the spike map of Purkinje cell was stable (Δg was 0.004 2 $\mu S/cm^2$). In order to describe the rabbit eye blink conditioned reflex phenomenon in detail, some indices including Interspike Period (IP), Quiescent Period (QP), Active Phase (AP) and Interburst Period (IB) were introduced to analyze the variation of Purkinje cell potential spike characters (Fig. 7).

Bursting is a dynamic state when a neuron repeatedly fires discrete groups or bursts of spikes. Such a burst is followed by a period of quiescence before the next burst occurs. Neuronal bursting plays important roles in the communication between neurons. Here 4 indexes were used to analyze the variation of Purkinje cell potential spike pattern in the process of eye blinking learning. As shown in Fig. 3A, Purkinje cell's spike pattern was in a disorder, so it was difficult to count the index IB. However, the width of each burst and the spike number in one burst could be obtained, and thus the index of IB was replaced by Mean Spike Numbers per Burst (MSN/B). Table 2 showed the results of rabbit eye blinking learning in the present cerebellar cortex network model.

In Table 2, g_0 represented the initial value of synaptic

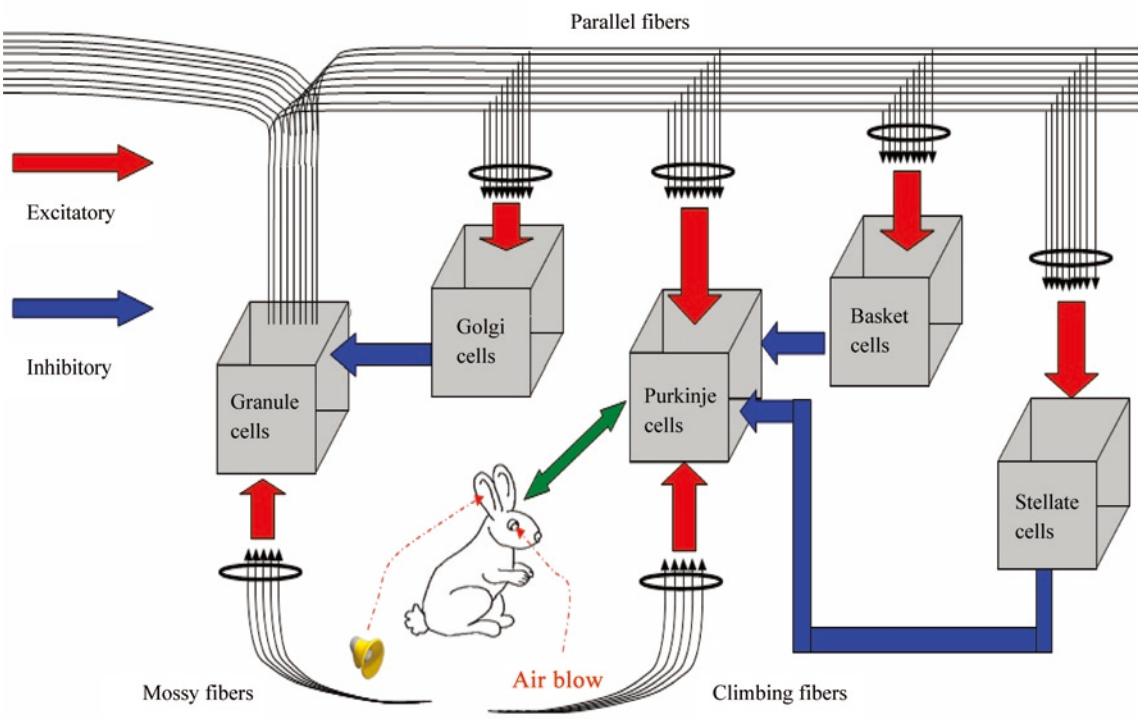

Fig. 6 The learning diagram of rabbit eye blink conditioned reflex. The specific process was as follows: when the bell rang, an air blow was made to rabbit's eyes on the right, and the rabbit's eyes would blink. Such process was repeated for several times. After repeated pairing of a ring tone with air blow, the tone would acquire the ability to elicit a blink on its own, which illustrated that the learning process of rabbit eye blink conditioned reflex was completed.

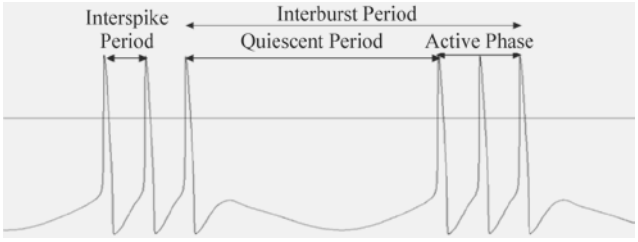

Fig. 7 The schema index of neuron spikes can be described by Interspike Period, Quiescent Period, Active Phase and Interburst Period.

strength between parallel fibers and Purkinje cells, while g_6 and g_7 represented the synaptic strength when learning process reached a stable state. g_7 (no CF) was obtained after removal of stimulation from climbing fiber when the learning times reached 7. It was shown that the value of IP was basically stable during learning, but the values of AP and QP were distinct from those in the case of no learning. In addition, AP was small while QP was large. When learning was completed, AP increased significantly, while QP decreased significantly, and MSN/B also changed obviously. The indices corresponding to g_6 and g_7 were very similar, indicating that after synaptic STDP learning was completed, the index character of Purkinje cell's potential spike was stable.

If the stimulation was removed from climbing fiber at this time, the value of IP was still stable, and the values of AP and QP were both basically similar between g_6

Table 2. The index character of Purkinje cell spikes

Synaptic strength	Index (ms)			
($\mu S/cm^2$)	IP	QP	AP	MSN/B
$g_0 = 0.3096$	309.75	225.388	84.363	54
$g_6 = 0.1725$	309.7375	204.1875	105.55	30
$g_7 = 0.1683$	309.7125	204.075	105.6375	28
$g_7 = 0.1683$ (No CF)	309.9375	204.5375	105.4	21

No CF indicated that stimulation on climbing fiber was removed after learning times reached 7. IP: Interspike Period. QP: Quiescent Period. AP: Active Phase. MSN/B: Mean Spike Numbers per Burst.

and g_7. MSN/B value showed a change, but it was only a little. Thus, the conclusion could be drawn that when the synaptic STDP learning from parallel fiber to Purkinje cell reached a stable state, removal of the afferent from climbing fibers could still keep the stability.

4 Discussion

In the present study, we established a cerebellar corical network model based on the actual cerebellar cortex structure. With the aid of neuronal compartment model and NEURON software, the action potential spike patterns of several main cells in the cerebellar cortex were analyzed and several theoretical results of cerebellar cortex system were obtained in this model.

The model results illustrate that Purkinje cell has different responses to the incoming message from different regions of brain. For the 2 inhibitory loops in the cerebellar network: the feedback loop of golgi cell and granule cell and the inhibitory loop of stellate/basket cell and Purkinje cell, we analyzed their corresponding effects: temporal focusing and spatial focusing, and found that the network model of cerebellar cortex is very close to the actual network. Most importantly, this model can reflect some characteristics of the cerebellar cortex structure. As the cerebellar cortex system experiments become more and more precise, the cell types in cerebellar cortex, the density of ion channels, the geometric morphology of dendrites and axons, and the specific locations of synaptic connections are confirmed. Theoretical descriptions of cerebellar cortex based on the compartment model are very close to the process of nervous system signal transduction. The model simulation results displayed the neural signal activities of neurons in cerebellum cortex.

Eye blink conditioned reflex is a classical conditioned reflex in motor learning. Take the rabbit eye blink conditioned reflex for example: the rabbit would make a blinking action in response to an air blow made to its eyes. However, after repeated pairing of a neutral stimulus, such as bell tone, with the blink-eliciting stimulus (blow), the bell tone will acquire the ability to elicit a blink on its own, the process of which is called eye blink conditioned reflex[2,31]. Thompson[35] and Yeo *et al.*[31] have found that the establishment of conditioned reflex has a close relationship with Purkinje cells in cerebellar cortex.

The signal of air blow transmits along the trigeminal nerve to brainstem, and excites the nucleus of facial nerve, the abducent nucleus, and anterior horn cells of the spinal cord, causing the action of blinking. The cerebellum is involved in conditioned reflex of eye blink. The air blow signal can reach the inferior olive nucleus, and transmits along the climbing fibers which proceed from inferior olive nucleus to cerebellar cortex, indicating that the transmission of air blow signals to cerebellar cortex is achieved via the parallel fibers[31-33]. The bell tone transmits via anteriornucleus and pontine nuclei, and reaches cerebellum through the mossy fibers, indicating that the transmission of bell tone to cerebellar cortex is achieved via the mossy fibers. Conditioned stimulus can activate the synapse of parallel fibers to Purkinje cell before unconditioned stimulus reaches cerebellum through climbing fibers, so the learning phenomenon would occur in parallel fiber-to-Purkinje cell synapses[31,34,35].

STDP is a temporally asymmetric form of Hebbian learning induced by tight temporal correlations between the spikes of pre- and postsynaptic neurons. As with other forms of synaptic plasticity, it is widely believed that STDP underlies learning and information storage in the brain, as well as the development and refinement of neuronal circuits during brain development[28].

With STDP, repeated presynaptic spike arrival a few milliseconds before postsynaptic action potentials leads to LTP of many types of synapses, whereas repeated spike arrival after postsynaptic spikes leads to LTD of the same synapse. The change of the synapse plotted as a function of the relative timing of pre- and postsynaptic action potentials is called the STDP function or learning window, and it varies among synapse types. The rapid change of the STDP function with the relative timing of spikes suggests the possibility of temporal coding schemes on a millisecond time scale.

Comparing the present simulation results with the description of rabbit eye blink conditioned reflex phenomenon reported previously[30-34], it can been seen that when the afferent from climbing fiber exists, the adaptation of

rabbit to eye blinking would gradually reach a stable state under STDP learning rule. This indicates that if the afferent from climbing fiber (air blow) is removed, the only afferent from mossy fiber (ring) can still produce the phenomenon of eye blinking, which may further illustrate the feasibility of the cerebellar cortex network model constructed in the present study.

Based on the STDP learning rule, stimuli of sound and air blow, which represent the mossy fibers and the climbing fibers, respectively, were applied. The learning adaptability of rabbit eye blink conditioned reflex phenomenon was verified in the present network model. It was found that after repeated pairing of sound stimulus with the air blow stimulus, the sound stimulus will acquire the ability to elicit a blink on its own. This further shows the accuracy of the present cerebellar cortical network model. The model simulation results confirmed the output signal stability of cerebellum cortex after STDP learning and that the network can execute the function of spatial and temporal focusing.

As the cerebellum cortex has simple network structures and possess many functions, it has attracted attention of theorists and modelers for many years. In this paper, we used models to understand the cerebellum's possible role in motor learning and control at the functional level. In fact, the cerebellum can be considered as multiple paired forward and inverse models[36]. Plasticity of parallel fiber synapses on interneurons and plasticity of interneuron-to-Purkinje cell synapses are connected with LTP or LTD[37]. All these basic properties of cerebellum may be further illuminated in our neural computational investigations.

Acknowledgements: This work was supported by the grants from National Natural Science Foundation of China (No. 10872069).

References:

[1] Yeo CH. Memory and the cerebellum. Curr Neurol Neurosci Rep 2004, 4: 87–89.

[2] Longstaff A. Instant notes in neuroscience. The United Kindom: Bios Scientific Publishers Limited, 2000.

[3] Carta M, Murru L, Barabino E, Talani G, Sanna E, Biggio G. Isoniazid-induced reduction in Gabaergic neurotransmission alters the function of the cerebellar cortical circuit. Neuroscience 2008, 154: 710–719.

[4] Bear MF, Connors BW, Paradios MA. Neuroscience: Exploring the Brain (2nd ed.). Maryland: Lippincott Williams & Wikins, 2001.

[5] Fabbro F. Introduction to language and cerebellum. J Neurolinguistics 2000, 13: 83–94.

[6] Ito M. Historical review of the significance of the cerebellum and the role of Purkinje cells in motor learning. Ann N Y Acad Sci 2002, 978: 273–288.

[7] Voogd J, Glickstein M. The anatomy of the cerebellum. Trends Neurosci 1998, 21: 370–375.

[8] Stevens JM, Kendall BE. Aspects of the anatomy of the cerebellum on computed topography. Neuroradiology 1985, 27: 390–398.

[9] Glickstein M, Sultan F, Voogd J. Functional localization in the cerebellum. Cortex 2011, 47(1): 59–80.

[10] Wolpert DM, Miall RC, Kawato M. Internal models in the cerebellum. Trends Cogn Sci 1998, 2(9): 338–347.

[11] de Gruijl JR, van der Smagt P, De Zeeuw CI. Anticipatory grip force control using a cerebellar model. Neuroscience 2009, 162: 777–786.

[12] Ito M. Cerebellar circuitry as a neuronal machine. Prog Neurobiol 2006, 78: 272–303.

[13] Van Der Giessen RS, Koekkoek SK, van Dorp S, De Gruijl JR, Cupido A, Khosrovani S, *et al.* Role of olivary electrical coupling in cerebellar motor learning. Neuron 2008, 58: 599–612.

[14] Tokuda IT, Han CE, Aihara K, Kawato M, Schweighofer N. The role of chaotic resonance in cerebellar learning. Neural Netw 2010, 23: 836–842.

[15] Cheron G, Servais L, Dan B. Cerebellar network plasticity: from genes to fast oscillation. Neuroscience 2008, 153: 1–19.

[16] Zeeuw CID, Hoebeek FE, Schonewille M. Causes and consequences of oscillations in the cerebellar cortex. Neuron 2008, 58: 655–658.

[17] Middleton SJ, Racca C, Cunningham MO, Traub RD, Monyer H, Knöpfel T, *et al.* High-frequency network oscillations in cerebellar cortex. Neuron 2008, 58: 763–774.

[18] Wikgren J, Nokia MS, Penttonen M. Hippocampo-cerebellar theta band phase synchrony in rabbits. Neuroscience 2010, 165: 1538–1545.

[19] Maex R, Schutter ED. Oscillations in the cerebellar cortex: a prediction of their frequency bands. Prog Brain Res 2005, 148: 181–188.

[20] Akemann W, Knopfel T. Interaction of Kv3 potassium channels and resurgent sodium current influences the rate of spontaneous firing of Purkinje neurons. J Neurosci 2006, 26(17): 4602–4612.

[21] Solinal S, Forti L, Cesana E, Mapelli J, Schutter ED, Angelo ED.

Computational reconstruction of pacemaking and intrinsic electroresponsiveness in cerebellar golgi cells. Front Cell Neurosci 2007, 1(2): 1–12.

[22] Solinas S, Forti L, Cesana E, Mapelli J, Schutter ED, Angelo ED. Fast-reset of pacemaking and theta-frequency resonance patterns in cerebellar Golgi cells: Simulations of their impact *in vivo*. Front Cell Neurosci 2007, 1(4): 1–9.

[23] Yamada WM, Koch C, Adams PR. Multiple channels and calcium dynamics. In: Koch C, Segev I (eds). Methods of neuronal modeling. Cambridge: MIT Press, 1987: 97–134.

[24] Migliore M, Shepherd GM. Dendritic action potentials connect distributed dendrodendritic microcircuits. J Comput Neurosci 2008, 24: 207–221.

[25] Carnevale T, Hines M. The NEURON Book. Cambridge: Cambridge University Press, 2006.

[26] Miyasho T, Takagi H, Suzuki H, Watanabe S, Inoue M, Kudo Y, *et al*. Low-threshold potassium channels and a low-threshold calcium channel regulate Ca^{2+} spike firing in the dendrites of cerebellar Purkinje neurons: a modeling study. Brain Res 2001, 891: 106–115.

[27] Rabinovich MI. Dynamical principles in neuroscience. Rev Modern Physics 2006, 78(4): 1213–1265.

[28] Bi GQ, Poo MM. Synaptic modification of correlated activity: Hebb's postulate revisited. Ann Rev Neurosci 2001, 24: 139–166.

[29] Nowotny T, Zhigulin VP, Selverston AI, Abarbanel HD, Rabinovich MI. Enhancement of synchronization in a hybrid neural circuit by spike-timing dependent plasticity. J Neurosci 2003, 23(30): 9776–9785.

[30] Katz DB, Tracy JA, Steinmetz JE. Rabbit classical eyeblink conditioning is altered by brief cerebellar cortical stimulation. Physiol Behav 2001, 72: 499–510.

[31] Yeo CH, Hesslow G. Cerebellum and conditioned reflexes. Trends Cogn Sci 1998, 2(9): 322–333.

[32] Nicholson DA, Sweet JA, Freeman JH. Long-term retention of the classically conditioned eyeblink response in rats. Behav Neurosci 2003, 117(4): 871–875.

[33] Rogers RF, Steinmetz JE. Contextually based conditional discrimination of the rabbit eyeblink response. Neurobiol Learn Mem 1998, 69: 307–319.

[34] Kelly TM, Zuo CC, Bloedel JR. Classical conditioning of the eyeblink reflex in the decerebrate-decerebellate rabbit. Behav Brain Res 1990, 38(1): 7–18.

[35] Thompson RF. The neurobiology of learning and memory. Science 1987, 233: 941–947.

[36] Wolpert DM, Miall RC, Kawato M. Internal models in the cerebellum. Trends Cogn Sci 1998, 2(9): 338–347.

[37] Jörntell H, Bengtsson F, Schonewille M, De Zeeuw CI. Cerebellar molecular layer interneurons-computational properties and roles in learning. Trends Neurosci 2010, 33(11): 524–532.

小脑皮层神经回路及其功能作用

汪雷，刘深泉

华南理工大学理学院数学系，广州 510640

摘要：目的 利用小脑的生理结构构造模拟小脑网络回路，研究小脑皮层不同神经细胞的电位发放、外界刺激对小脑皮层细胞的影响以及各类细胞电位发放模式等。**方法与结果** 利用神经元的多房室模型和NEURON软件，研究不同输入刺激对蒲肯野细胞电位发放的影响。对颗粒细胞–高尔基细胞的反馈抑制回路对蒲肯野细胞的时间聚焦以及平行纤维–篮状/星状细胞局部抑制回路对蒲肯野细胞的空间聚焦现象进行了验证。运用施加运动学习的小脑网络模型研究兔子眨眼的条件反射现象，用模型的电位发放指标反映学习后兔子眨眼的实验现象。当刺激信号从攀状纤维输入时，通过精确放电时间依赖的突触可塑性学习，兔子眨眼的适应作用逐渐达到稳定状态。 **结论** 本文构造的小脑皮层网络真实可靠。模型的数值结果证实，小脑皮层经过精确放电时间依赖的突触可塑性学习后，输出信号稳定，可以执行时间聚焦和空间聚焦的功能。

关键词：网络模型计算；小脑皮层；时间聚焦；空间聚焦；精确放电时间依赖的突触可塑性；眨眼条件反射